

## Strength, Rapid Chloride Penetration and Microstructure Study of Cement Mortar Incorporating Micro and Nano Silica

Rishav Garg<sup>1,\*</sup>, Manjeet Bansal<sup>2</sup>, and Yogesh Aggarwal<sup>3</sup>

<sup>1</sup> Research Scholar, I.K. Gujral Punjab Technical University, Kapurthala-144603 (India)

<sup>2</sup> Giani Zail Singh Campus College of Engineering & Technology, Bathinda-151001 (India)

<sup>3</sup> National Institute of Technology, Kurukshetra-136119 (India)

\*E-mail: [rishavgarg77@yahoo.com](mailto:rishavgarg77@yahoo.com)

Received: 10 February 2016 / Accepted: 27 February 2016 / Published: 1 April 2016

---

This paper presents the strength, rapid chloride penetration and microstructure study of cement mortar incorporating micro-silica (MS), nano-silica (NS) and micro-silica with optimized content of nano-silica (MS+NS) as a partial replacement of cement. The hardened properties of the mortar such as compressive strength and split tensile strength of all the specimens has been determined at the age of 28, 56, 90 and 180 days. Quadratic model and ANOVA analysis has been carried out to determine the optimized content of NS. Further, durability properties of all the specimens have also been determined in terms of carbonation test. The microstructure of the specimens has been determined by SEM-EDX studies. The results reveal the enhanced strength, durability and improved microstructure of mortar specimens with proper combination of micro and nano silica resulting in better performance as compared to conventional specimens.

---

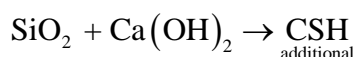
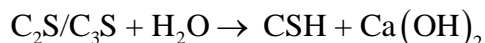
**Keywords:** Microstructure, rapid chloride penetration, strength, nano-silica, micro-silica

### 1. INTRODUCTION

The microstructure and strength of cement mortars is significantly affected by the water/binder ratio, and chemical composition [1]. The chief concern of practicing researchers and civil engineers is aimed at improvement of the microstructure and strength of cementitious materials along with minimizing the use of conventional resources leading to sustainable construction practices. In this context, supplementary cementitious materials (SCMs) as a partial replacement of cement have been investigated extensively in recent years including metakaolin [2], nano-TiO<sub>2</sub> [3], nano-Al<sub>2</sub>O<sub>3</sub> and nano-Fe<sub>2</sub>O<sub>3</sub> [4]. SCMs improve the performance of cementitious materials by improving their

microstructure, chemical nature and mechanical properties in the fresh and hardened stages leading to extended service life. The pozzolanic materials such as micro-silica (MS) and nano-silica (NS) are gaining significant attention due to their better performance as compared to other additives [5-7].

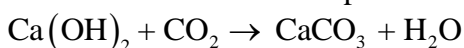
The cement hydration produces a sulphate rich solution due to dissolution of the gypsum ( $\text{CaSO}_4 \cdot 2\text{H}_2\text{O}$ ) and sulphates present in the anhydrous cement clinkers. This results in the conversion of aluminate ( $3\text{CaO} \cdot \text{Al}_2\text{O}_3$ ) to ettringite ( $\text{CaO} \cdot 3\text{Al}_2\text{O}_3 \cdot 3\text{CaSO}_4 \cdot 32\text{H}_2\text{O}$ ) primarily responsible for first setting. The hydration of alite ( $\text{C}_3\text{S}$  or  $3\text{CaO} \cdot \text{SiO}_2$ ) and belite ( $\text{C}_2\text{S}$  or  $2\text{CaO} \cdot \text{SiO}_2$ ) produces portlandite or calcium hydroxide [ $\text{Ca}(\text{OH})_2$ ] or CH and calcium silicate hydrates or CSH gel. The reaction can be represented as follows:



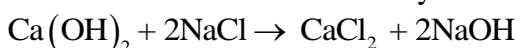
The large CH crystals with small van der Waals forces do not contribute towards strength and rather, reduce the performance of the cementitious material on dissolution in sulphate and acidic waters. The fine crystalline CSH gel particles enhance the strength of the cementitious material by occupying the voids in the cement matrix [7].

The incorporating effect of MS and NS is tri-fold due to pozzolanic action, nucleation effect and filler effect. The amorphous silica particles of MS and NS react with the CH produced by cement hydration resulting in the formation of additional CSH gel that fills the voids in the cement matrix. The fine particles of MS and NS act as nucleation sites due to high surface area leading to crystallization of CSH gel at the space available in the voids and the grain surface. During this process, the cement hydration gets accelerated and the availability of CH increases for further reaction with silica particles leading to consumption of CH. As a result, the microstructure of the cement matrix gets more dense and homogeneous with enhanced strength. The filler effect of the fine particles replaces the water molecules present in the interfacial zone (ITZ) and the voids of the cement matrix, forming a uniform structure with less permeability and increased packing [8].

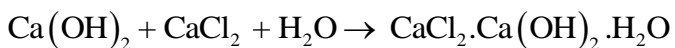
The strength & durability of the mortar depend mainly on the quality & quantity of the matrix. The properties of the cement mortar keep on changing with time due to the electrochemical interactions of the cement matrix with aggressive environment and the microstructure of the mix. The durability of the cementitious materials can be measured in terms of carbonation and rapid chloride penetration test. Carbonation is the reaction of atmospheric carbon dioxide with water present in mortar to form carbonic acid that further reacts with the hydrates present in the cement matrix to form carbonates. The reaction can be represented as follows:



Carbonation decreases the pH of the pore fluid and decreases the strength of the cement matrix due to consumption of hydrates [9]. When cementitious materials come in contact with corrosive environment containing aggressive ions such as chloride ions, deterioration takes place due to the reaction of chloride ions with calcium hydroxide  $\text{Ca}(\text{OH})_2$  in the cement matrix.



This reaction further leads to the formation of expansive products responsible for destruction of the material:



The use of pozzolanic materials can lead to a decrease in carbonation and permeability leading to increased durability of the cementitious materials. This paper presents the effect of incorporation of micro-silica/nano-silica (MS/NS) and micro-silica in presence of nano-silica (MS+NS) as a partial replacement of cement on the split tensile strength, compressive strength, rapid chloride penetration, carbonation and microstructure of mortar specimens at 28, 56, 90 and 180 days. The paper is aimed to provide a deep insight on the participation of the two pozzolanic materials- MS and NS and the optimization of NS content for use in the sustainable construction development due to improved performance of the cementitious materials in terms of enhanced strength and lesser chloride penetration. The observed behavior has been critically analyzed in terms of pozzolanic behavior of MS and NS .

## 2. EXPERIMENTAL METHODS

### 2.1. Materials

Ordinary Portland Cement (OPC) 43 grade with standard consistency of 29.0% complying with Indian Standard IS: 8112-2013 was used for preparation of all the specimens.

**Table 1.** Physical characteristics and Chemical composition\* (%) of the materials

	Specific Gravity	Average particle size	Specific Surface (m <sup>2</sup> /g)	CaO	SiO <sub>2</sub>	Al <sub>2</sub> O <sub>3</sub>	FeO	MgO	TiO <sub>2</sub>	L.O.I
OPC	3.15	16 μm	0.31	62.2	20.82	5.2	3.35	2.65	0.27	3.09
NS	1.31	20 nm	140	-	99.9	-	-	-	-	2.8
MS	2.21	<1 μm	13-30	0.05	98	0.03	0.02	0.10	0.03	<2

\*Ambuja Cement

The cement particles had the fineness equal to 310 m<sup>2</sup>/kg and specific gravity equal to 3.15. Standard Ennore sand was used after standard sieve analysis was performed in compliance with IS: 2386 (Part-I)-1963. Micro-silica (MS) with bulk density 630 kg/m<sup>3</sup> and colloidal nano-silica (NS) with solid strength 30% was used as such without any modification. The physical characteristics and chemical composition of the materials used has been provided in table 1. The water used to prepare all specimens was in accordance to IS: 456-2000.

2.2. Methodology for Mix Proportion and testing of the specimens

The specimens for each mix with water/binder ratio (W/B) of 0.45 and cement/standard sand weight ratio (C/S) of 1:3 were prepared by mechanical mixing (IS: 2250-1981). The amount of water to prepare the specimens with NS was reduced according to the specific amount of water present in colloidal NS. The Control mix (CMS) was prepared without replacement of cement with MS and NS. The mortar paste was prepared by partial replacement of cement by MS with dosage varying @ 5% from 5% to 20 % (Specimens MM1 to MM4) and NS with dosage varying @ 0.25% from 0.5 % to 1.25% (Specimens MN1 to MN4). The specimen containing NS with maximum split tensile strength at 28 days was selected for optimum dosage and a combination of MS with content varying @ 5% from 5% to 20 % at fixed optimum NS (1%) was used to replace cement (Specimens MNM1 to MNM4). The mix proportion of the specimens has been shown in table 2.

**Table 2.** Mix proportion of the specimens in terms of weight of materials

Specimen	Water (g)	Cement (g)	Sand (g)	W/B	MS (g)	NS (g)
CMS	90.000	200.0	600	0.45	-	-
MM1	90.000	190.0	600	0.45	10	-
MM2	90.000	180.0	600	0.45	20	-
MM3	90.000	170.0	600	0.45	30	-
MM4	90.000	160.0	600	0.45	40	-
MN1	87.670	199.0	600	0.45	-	1.0
MN2	86.500	198.5	600	0.45	-	1.5
MN3	85.340	198.0	600	0.45	-	2.0
MN4	84.175	197.5	600	0.45	-	2.5
MNM1	85.340	188.0	600	0.45	10	2.0
MNM2	85.340	178.0	600	0.45	20	2.0
MNM3	85.340	168.0	600	0.45	30	2.0
MNM4	85.340	158.0	600	0.45	40	2.0

For each mix, cylindrical specimens of 100 mm x 200 mm were prepared. The specimens were demoulded after 24 hours and cured in water at 27±2°C for 28, 56, 90 and 180 days. The split tensile strength of the specimens,  $f_{ct}$  was determined in accordance with the IS 5816-1999 by using the equation:

$$f_{ct} = \frac{2P}{\pi dl} \text{-----(1)}$$

Where,  $P$  is the load applied to the specimen,  $d$  is the diameter (100 mm) and  $l$  is the length of the specimen (200 mm).

For compressive strength studies, the cubes of 7.06 cm (IS: 10080 - 1982) were cast and immersed in water tank. After curing under desired conditions, three mortar specimens (for each mix) were retrieved from the tank and compressive strength was analyzed at 28, 56, 90 and 180 days (IS: 4031(Part 6)-1988).

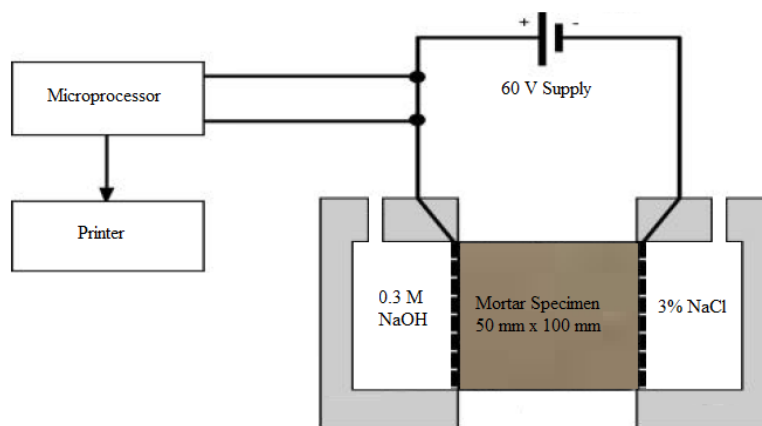


**Figure 1.** Rapid Chloride Permeability Test Setup

For rapid chloride penetration resistance test (RCPT), the 100 mm x 200 mm cylinders were cast and sliced into 50 mm x 100 mm (according to ASTM C 1202- 97). The amount of electrical current passed through the sliced specimens was monitored for a 6-h period by impressing the potential difference of 60 V as shown in figure 1. One end of the specimen was immersed in a 3% NaCl solution and the other end was immersed in a 3 M NaOH solution. The total charge, in coulombs, was calculated by correlation with the resistance of the sliced specimen to chloride ion penetration.

Carbonation test was carried out by determination of the depth of color less region using phenol- phthalein indicator. The freshly split specimens was thoroughly cleaned followed by spraying with the phenolphthalein pH indicator (95.0% by volume in ethanol). The average depth 'D' of the colorless region was measured immediately after spraying the indicator at three points in a direction perpendicular to the two edges of the split side.

For microstructure analysis, hydration of the mortar specimens was stopped after curing at the desired days. The microstructure analysis of the specimens was performed using scanning electron microscopic (SEM-EDX) studies on gold coated specimens through Philips XL20 Scanning Electron Microscope.

### 3. RESULTS AND DISCUSSION

#### 3.1. Split tensile strength

The split tensile strengths of CMS and mortar specimens incorporating MS, NS and MS+NS had been determined at a curing age of 28, 56, 90 and 180 days. The split tensile strength of specimens

incorporated with NS has been found to be more as compared to the specimens incorporated with MS as shown in figure 2. This observation can be attributed to the enhanced reaction of NS particles with the generated C-S-H gel resulting in more densification of the cement matrix. Further, it was found that the mortar specimen incorporated with 1% NS developed maximum increase in the split tensile strength at 28 age (Standard age), hence 1% NS was selected as the optimum percentage for incorporation of specimens with MS+NS.

**Table 3.** Split tensile and Compressive strength of the specimens with increasing curing age

Specimen	Consistency (%)	% increase in Split tensile strength				% increase in Compressive strength			
		28 days	56 days	90 days	180 days	28 days	56 days	90 days	180 days
MM1	32	7	10	8	11	10	6	5	6
MM2	34	10	11	10	13	16	11	15	16
MM3	37	12	13	16	18	20	15	17	15
MM4	38	11	11	14	15	18	12	12	10
MN1	31	22	19	20	22	17	10	5	9
MN2	33	21	20	18	24	21	12	9	9
MN3	34	23	22	21	28	24	14	12	11
MN4	34	21	21	20	25	23	10	8	7
MNM1	37	26	30	30	31	36	29	26	29
MNM2	38	26	33	33	34	53	39	37	34
MNM3	38	27	32	31	33	46	36	38	39
MNM4	40	26	31	31	30	42	33	32	30

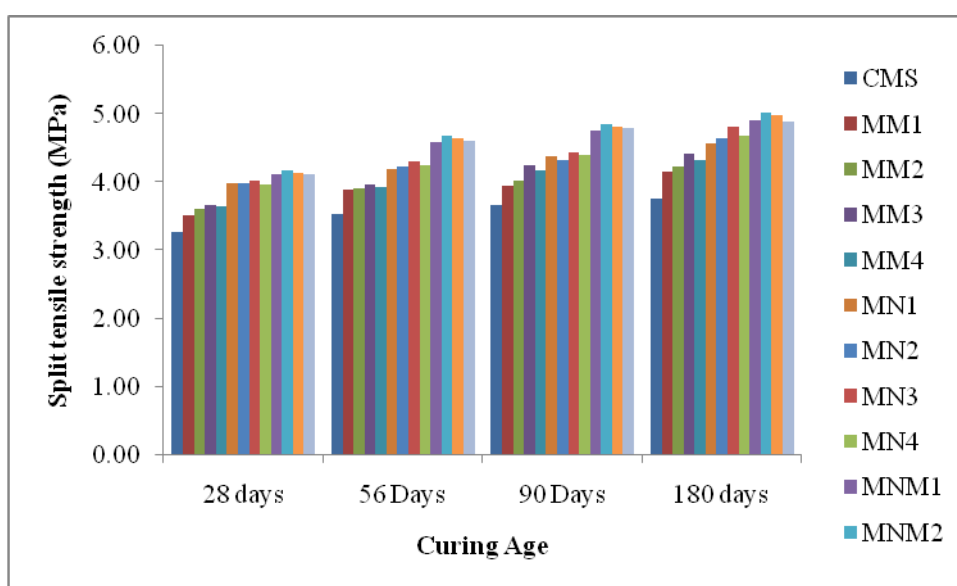


**Figure 2.** Split Tensile Strength of the specimens with increasing curing age

These specimens resulted in further increase in split tensile strength as compared to earlier specimens due to better distribution of the particles and enhanced filler effect leading to increase of the split tensile strength. However, all the specimens showed an increase of the split tensile strength only up to a particular percentage of the incorporated NS/MS and MS+NS particles and decreased afterwards. This observation can be attributed to the agglomeration tendency and increased friction of NS and MS particles with increase in their incorporation percentage. As a result, the pozzolanic particles may not show their pozzolanic behavior leading to a decrease in densification of the matrix and split tensile strength [13, 15, 16].

3.2. Isoresponse curves for Split tensile strength

**Table 4.** Quadratic Coefficient model for split tensile strength with increasing curing age

Curing age (Days)	Coefficients					
	$a_o$	$a_1$	$a_2$	$a_{11}$	$a_{22}$	$a_{12}$
28	+4.17	+0.083	+0.22	-0.11	-0.35	-0.083
56	+4.60	+0.15	+0.32	-0.22	-0.32	-0.025
90	+4.77	+0.20	+0.31	-0.20	-0.35	-0.059
180	+4.98	+0.14	+0.31	-0.21	-0.39	-0.14

**Table 5.** Annova Analysis for split tensile strength with increasing curing age

Source of Variance	Sum Sq.	dF	Mean Sq.	F	P	R <sup>2</sup>	R <sup>2</sup> adj.
Split tensile strength at 28-Days							
Model	0.96	5	0.19	75.62	< 0.0001	0.9818	0.9688
Residual	0.011	6	0.001751				
Split tensile strength at 56-Days							
Model	1.51	5	0.30	126.65	< 0.0001	0.9891	0.9813
Residual	0.017	7	2.383E-003				
Split tensile strength at 90-Days							
Model	1.58	5	0.32	56.46	< 0.0001	0.9758	0.9585
Residual	0.039	7	5.580E-003				
Split tensile strength at 180-Days							
Model	1.67	5	0.33	99.79	< 0.0001	0.9899	0.9826
Residual	0.023	7	3.357E-003				

Various models based upon the quadratic response surface were developed using Design-Expert software for the specimens to estimate R<sup>2</sup>, the correlation coefficient at the curing age of 28, 56, 90 and 180 days [14]. The Quadratic model was found to best fit among the all models.

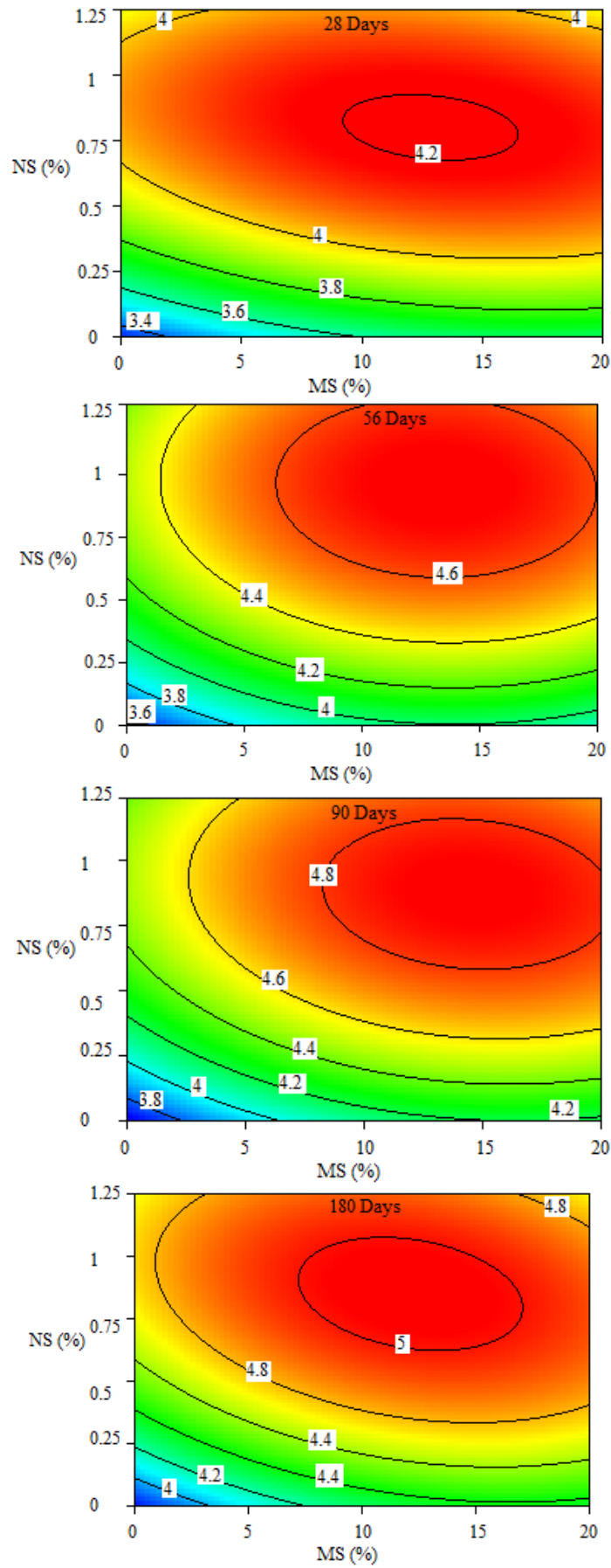


Figure 3. Isoresponse curves for Split Tensile Strength with increasing curing age

The content percentage of MS, NS and MS+1%NS at all the studied curing ages was correlated for split tensile strength of specimens in the quadratic model to represent the strength ( $Y$ ) as in Eq. (2).

$$Y = a_o + a_1x_1 + a_2x_2 + a_{11}x_1^2 + a_{22}x_2^2 + a_{12}x_1x_2 \text{ -----(2)}$$

where  $x_1$  is the content dosage of MS,  $x_2$  is the content dosage of NS,  $a_o$ ;  $a_1$ ;  $a_2$ ;  $a_{11}$ ;  $a_{22}$  and  $a_{12}$  are the model coefficients.

The obtained values of the coefficient of determination ( $R^2$ ) and the model coefficients have been given in table 4. The isoresponse curves of the split tensile strength have been illustrated in figure 3 to show the mutual interactions of the components in the ternary system in the studied domain.

The isoresponse curves for 28 days show contour patterns with maxima corresponding to 15% MS in presence of 1% NS dosage for partial replacement of cement. However, the contour patterns change significantly and show similar contour patterns for 56, 90 and 180 days indicating the similar trends of increase in strength. The results are in good agreement with the observations in split tensile strength and compressive strength measurements.

In all these curves, the stationary point for maxima is obtained at 10% MS in presence of 1% NS dosage for partial replacement of cement with around 34% increase in split tensile strength. Thus, the results reveal the optimum dosage for partial replacement of cement as 10% MS in presence of 1% NS in terms of later age increase in split tensile strength. The model results have been verified by analysis of variance (ANNOVA) and were found in good accordance. The results obtained by ANNOVA analysis have been summarized in table 5. The higher value of  $R^2$ , as compared to  $R^2$  adjusted value, confirm the validity of the results in the statistical model.

### 3.3. Compressive strength

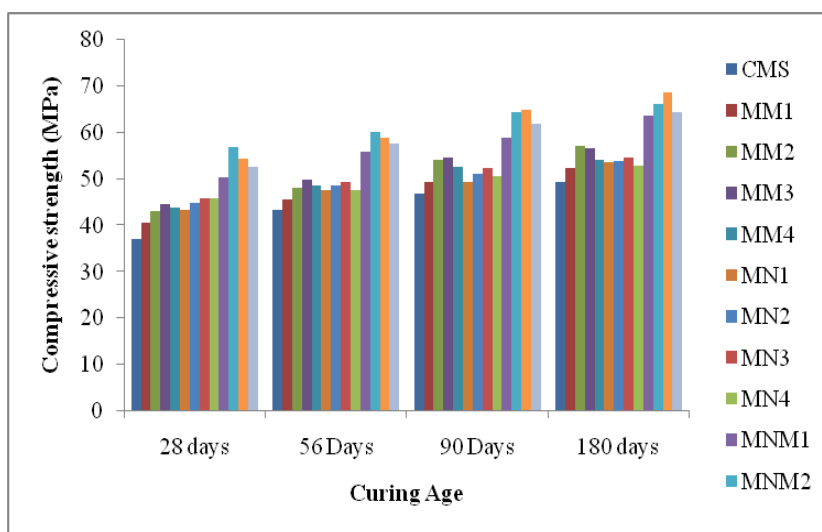


**Figure 4.** Compressive strength of the specimens with increasing curing age

The compressive strengths of CMS and mortar specimens on partial replacement of cement with MS, NS and MS+NS was determined at a curing age of 28, 56, 90 and 180 days. Figure 4 shows a

gradual increase in the compressive strength of mortar specimens, on partial replacement of cement with MS, NS and MS+NS as compared to CMS. The specimens containing NS developed better compressive strength than the specimens containing MS. This observation can be attributed to the better pozzolanic action of NS as compared to MS due to its greater silica content and finer particles with uniform dispersion and greater packing ability. It results in efficient generation of C-S-H gel and densification of the cement matrix leading to enhanced compressive strength [17, 18]. The specimens with MS+1% NS developed further enhanced compressive strength as compared to other specimens (with and without MS or NS). This observation indicates the better pozzolanic action of MS in presence of NS and can be due to better filler effect and further distribution of the particles in the remaining voids leading to homogeneous cement matrix and increased compressive strength.

All the specimens developed compressive strength only up to a particular dosage of MS/NS and MS+NS and after that a decrease was observed, in consistence with the work reported in literature [17-19]. This trend in compressive strength can be linked to the agglomeration tendency of NS particles and increase in friction between particles of MS/NS and MS+NS with increase in dosage of partial replacement leading to decreased pozzolanic behaviour resulting in lesser densification of the matrix and decreased compressive strength [1].

### 3.4. Durability Studies

Durability of cement mortar is its ability to resist against chemical, weathering, abrasion or any other process of deterioration so that it can retain its original identity, quality & serviceability during its whole designated life when exposed to atmosphere for which it is being prepared. Many chemical, electrochemical & physical processes are responsible to cause cracking in cement mortar & hence affecting its durability. The durability of the cement matrix can be enhanced by incorporation with pozzolanic materials as studied by researches [9].

#### 3.4.1. Rapid Chloride Permeability (RCPT) Test

Rapid chloride permeability test is a measure of the rate of penetration of the chloride ions in the cement matrix exposed to saline environment and is measured as total charge passed through the specimens, in coulombs [10].

Figure 5 reports the RCPT values of all the specimens obtained on analysis of all the mortar specimens at the age of 28, 56, 90 and 180 days. The permeability of CMS was observed to be greater than the mortar specimens incorporated with MS/NS and MS+NS and decreased with increase in incorporation content of MS/NS upto certain extent.

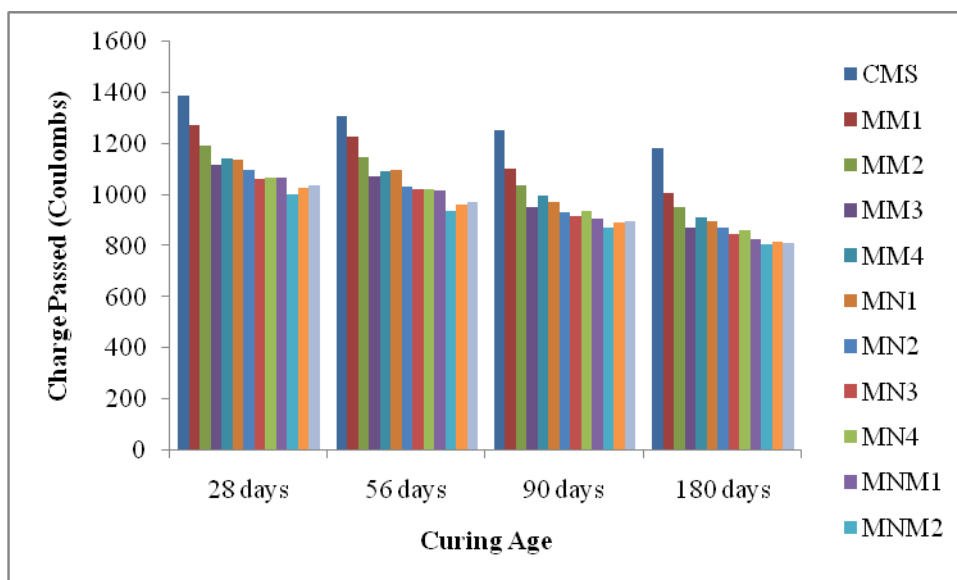


Figure 5. RCPT values of the specimens with increasing curing age

Table 6. RCPT and Carbonation results with increasing curing age

Specimen	Ca/Si ratio	% decrease in RCPT				Depth of carbonation in mm		Carbonation coefficient	
		28 days	56 days	90 days	180 days	90 days	180 days	90 days	180 days
MM1	1.44	8	6	12	15	2.35	3.10	1.36	1.27
MM2	1.16	14	12	17	20	2.30	2.80	1.33	1.14
MM3	0.39	20	18	24	26	2.20	2.70	1.27	1.10
MM4	0.61	18	17	20	23	2.22	2.65	1.28	1.08
MN1	0.72	18	16	22	24	1.85	2.25	1.07	0.92
MN2	0.25	21	21	26	26	1.83	2.10	1.06	0.86
MN3	0.15	24	22	27	28	1.75	2.00	1.01	0.82
MN4	0.20	23	22	25	27	1.80	2.00	1.04	0.82
MNM1	0.14	23	22	28	30	1.65	1.85	0.95	0.76
MNM2	0.09	28	28	30	32	1.55	1.80	0.89	0.73
MNM3	0.10	26	26	29	31	1.60	1.90	0.92	0.78
MNM4	0.14	25	26	29	31	1.65	1.95	0.95	0.80

The maximum decrease of 20%, 18%, 24%, 26% at 28, 56, 90 and 180 curing days respectively was observed in specimen with 15% MS and a decrease of 24%, 22%, 27%, 28% at 28, 56, 90 and 180 curing days respectively was observed in specimen with 1% NS (Table 6). However, in case of the specimens incorporated with MS+1% NS, the maximum decreased obtained was 28%, 28%, 30%, 32% at 28, 56, 90 and 180 curing days respectively. The permeability of cement matrix depends upon the pore structure and the extent of hydration of the cement matrix. The generated CSH gel due to the pozzolanic reaction and the filler effect of MS and NS particles results in pore reduction in the cement

matrix and decreases its permeability. Further, due to greater pozzolanic action and filler effect of NS particles, the permeability of the mortar specimens incorporated with NS decreases more. However, it was observed that the permeability of specimens incorporated with MS+1% NS decreased further. This observation can be attributed to the better pozzolanic action of MS in presence of NS. The increase in permeability in specimens incorporated with MS+1% NS can be due to the agglomeration of MS and NS particles at high concentration leading to deterioration in pore structure [11].

### 3.4.2 Carbonation

The carbonation test was carried out at curing ages of 90 days & 180 days and it was observed that the depth of carbonation increases with the curing age. Table 6 reports the carbonation depth of all the specimens at 90days and 180days of curing age. It is evident from the figure 6 that carbonation depth decreases with incorporation of MS/NS and MS+NS due to better packing and less porosity. The square root‘t’ law holds as good with the observed values as depth of carbonation varies linearly with square root of time.

$$D = K\sqrt{t}$$

Where t is time in months and K is carbonation coefficient. The value of K reported in table 6, didn’t exceed 1.5 conforming the resistance of specimens against carbonation [12]. The reduction in average pore size of the material decreases the carbonation. The increase in carbonation of cement mortar can be linked to the formation of additional CSH due to the reaction of pozzolanic particles with calcium hydroxide in the mortar matrix leading to reduction in pores with enhanced packing effect with formation of denser and stronger cement matrix [9]. The carbonation depth of the cement mortar containing NS is lower than in MS because of more densification of cement matrix in presence of finer NS particles. The combined effect of MS+NS resulted in lesser carbonation depth in comparison to MS and NS because of better filler effect & good dispersion of NS particles in presence of MS.

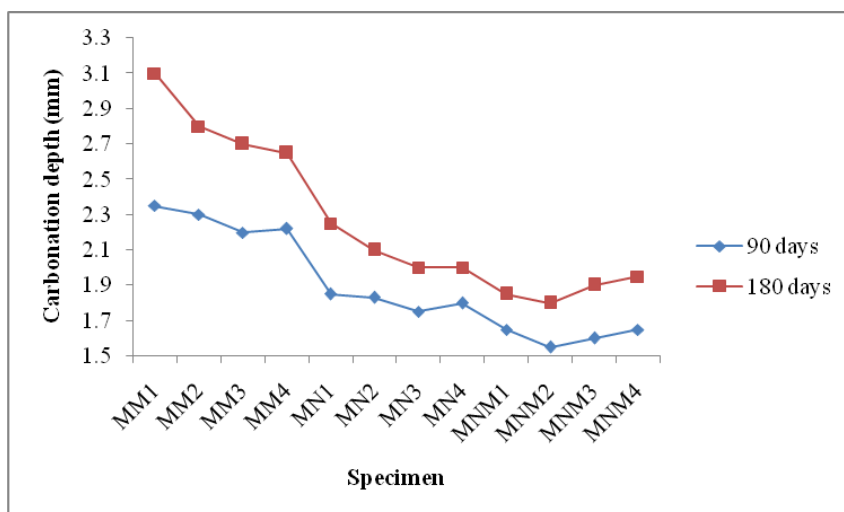


Figure 6. Carbonation depth of the specimens at 90 and 180 days

The results confirm the better development of cement matrix in presence of MS+NS & better performance in terms of resistance towards carbon dioxide.

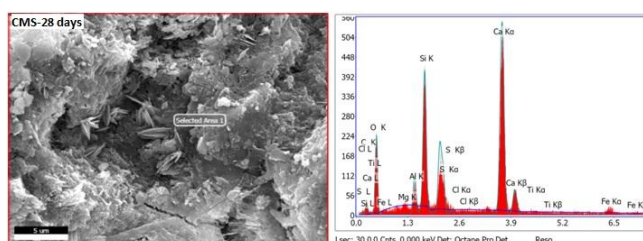
### 3.5. SEM-EDX analysis

The microstructure of the specimens was determined by SEM studies for correlation with the strength studies. The micrographs of all the mortar specimens, without and with incorporation of MS/NS and MS+NS, have been given in Fig.7-8. The micrographs obtained by SEM analysis provide the microstructure of a mortar specimen that can be characterized into the following distinct phases:

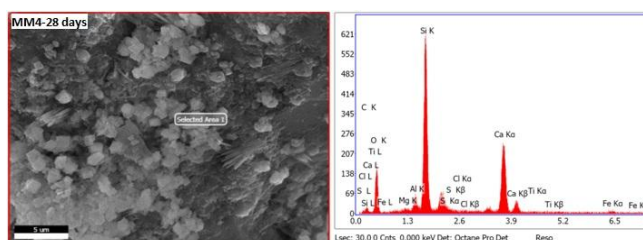
- (i) The pores in the cement matrix as the darkest phase
- (ii) The needles and hexagonal plates of calcium hydroxide as the less darker phases
- (iii) The unreacted anhydrous cement grains as the brightest phases
- (iv) The ettringite and C-S-H gel as massive fibroid/crown like phase or small needles.

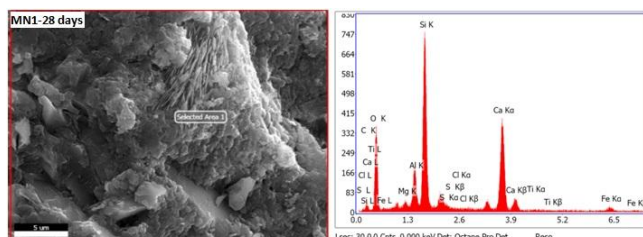
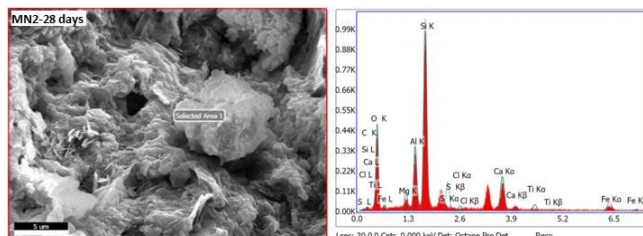
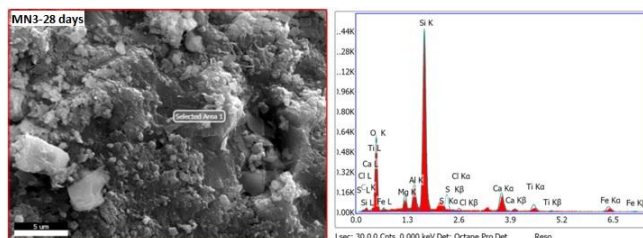
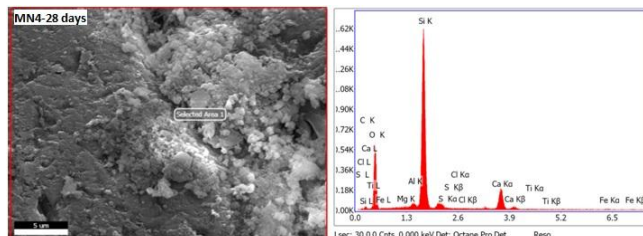
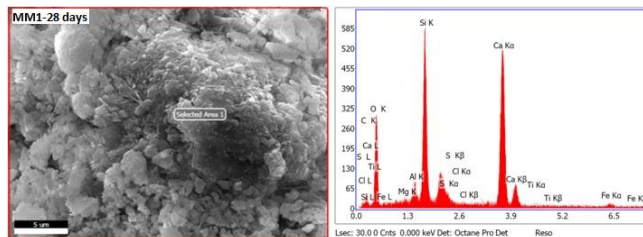
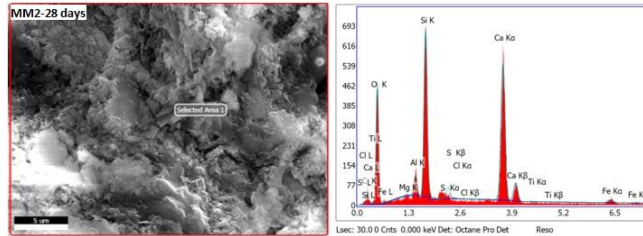
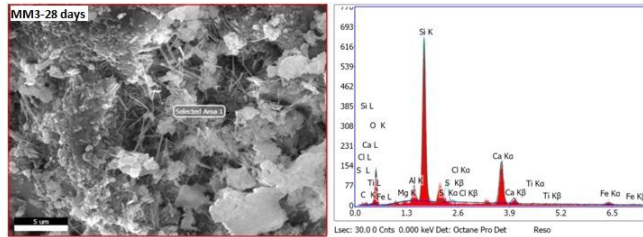
Small needle of calcium hydroxide with interconnected capillary pores were observed in the microstructure of the mortar specimens without incorporation of MS/NS. On the other hand, the microstructure of the mortar specimens with incorporation of MS showed comparatively lesser needle of calcium hydroxide with presence of C-S-H gel flakes resulting in an increase in the split tensile strength.

However, the microstructure of the specimens incorporated with NS was observed to be more homogeneous, dense and compact with greater proportion of C-S-H gel but reduced calcium hydroxide in consistence with the split tensile strength studies. The specimens incorporated with MS+NS showed further improvement in microstructure with densification of the cement matrix due to the presence of greater C-S-H fibroid/crown like phases and immense reduction in pores [20]. Thus, the microstructural development of the cement matrix incorporated with MS in presence of NS leads to enhanced split tensile and compressive strength due to the reinforcement of the cement matrix of the mortar specimens [21].



**Figure 7.** SEM-EDX micrographs of mortar specimens without replacement of cement





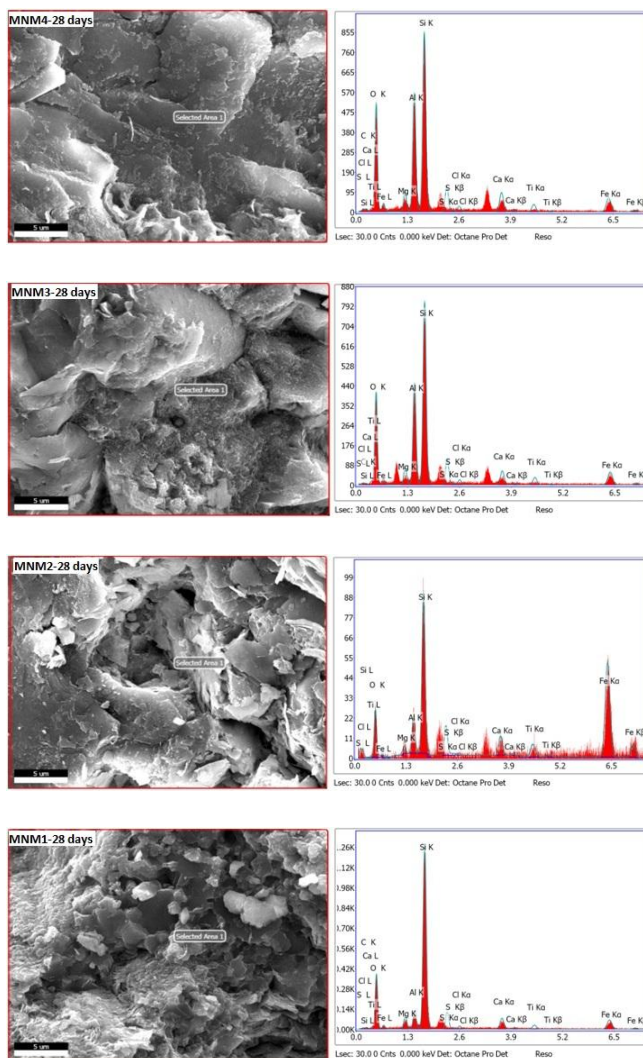


**Figure 8.** SEM-EDX micrographs of mortar specimens with partial replacement of cement

The observed decrease in split tensile strength and compressive strength at a particular incorporation amount of MS/NS and MS+NS is well attributed to the formation of agglomerates of the pozzolanic particles observed in the SEM micrographs [18].

EDX analysis of the specimens was used to determine the Ca/Si ratio at various regions (Table 6). The Ca/Si ratio greater than 1.7 indicate the presence of CH while the Ca/Si ratio smaller than 1.7 indicate the presence of CSH. The Ca/Si ratio  $\approx 3$  correspond to the partially hydrated zones of calcium trisilicate and the Ca/Si ratio  $\gg 3$  infer the zones rich in CH. As the Ca/Si ratio increases, the amount of CH increases while the amount of CSH increases with decrease in the Ca/Si ratio [22]. The cement matrix can be characterized into distinct phases depending upon the range of Ca/Si ratio:

- (i) C-S-H gel with Ca/Si ratio less than 2.0
- (ii) C-S-H gel particles with precipitated CH between the grains with Ca/Si ratio  $\approx 2.0$
- (iii) large proportion of CH with Ca/Si ratio  $\gg 5$
- (iv) a tobermorite-like phase containing congruent C-S-H with Ca/Si ratio  $\approx 1.0$

The results are in consistence with strength studies and SEM observations. The low Ca/Si ratio ( $\approx 2.0$ ) in plain cement mortars indicates the presence of CSH at 28 days. The Ca/Si ratio was found to decrease in all the specimens containing MS and/or NS corresponding to the microstructure development. Further, the specimens with MS+NS exhibited comparatively lower Ca/Si ratio corresponding to higher CSH content leading to densification of the matrix. However, the variability of the Ca/Si ratio and hence, the compositional difference of the CSH content in the specimens can be inferred to the heterogeneous reaction on the particle surface due to formation of agglomerates at higher content of MS/NS.

#### 4. CONCLUSION

The microstructure and strength correlation of cement mortars on partial replacement of cement with MS, NS and MS+1%NS has been carried out on the basis of split tensile strength, compressive strength, rapid chloride penetration, carbonation and SEM-EDX analysis of cement mortar specimens. The split tensile strength and compressive strength of the cement mortar specimens with MS, NS and MS+1%NS at the curing age of 28, 56, 90 and 180 days was found to be higher as compared to conventional mortar specimens. These results were attributed to the pozzolanic action and filler effect that was found to accelerate in case of specimens with NS in comparison to that containing MS and further increased in specimens with MS+NS. This also contributed to increased durability of these specimens in terms of decreased RCPT values and carbonation depth. Further, the isoresponse curves indicate the optimum content dosage for partial replacement of cement with 10% MS in presence of 1% NS for better performance in terms of split tensile strength. The formation of C-S-H hydrates was confirmed in SEM-EDX studies with the improvement of microstructure of the specimens with MS, NS and MS+1%NS. Thus, the increase in split tensile strength & compressive strength with decrease in RCPT values and carbonation depth of the mortar specimens containing MS+NS in comparison to mortar specimens without MS and/or NS is well correlated to the improvement in the microstructure of the specimens. No doubt, use of proper combination of MS and NS can improve physical and electrochemical behavior of cementitious materials leading to sustainable construction practices.

#### ACKNOWLEDGEMENT

The authors are grateful to acknowledge all the support extended by I.K Gujral Punjab Technical University, Kapurthala during the tenure of this study.

#### References

1. G.A. Rao, *Cem. Concr. Res.*, 33 (2003) 1765–1770.
2. Morsy MS, Al-Salloum Y, Almusallam T, Abbas H., *J. Therm. Anal. Calorim.*, 116 (2014) 845–852.
3. D. Feng, Xie N, Gong C, Leng Z, Xiao H, H. Li, *Ind. Eng. Chem. Res.*, 52 (2013) 11575-11582.
4. Oltulu M, Şahin R., *Mater. Sci. Eng. A*, 528 (2011) 7012–7019.

5. L. Senff, D. Hotza, W.L. Repette, V.M. Ferreira, J. Labrincha, *Constr. Build. Mater.*, 24 (2010) 1432-1437.
6. S. Abd.el.aleem, M. Heikal, W.M. Morsi, *Constr. Build. Mater.*, 59 (2014) 151–160.
7. L. Senff, D. Hotza, W.L. Repette, V.M. Ferreira, *Adv. Appl. Ceram.*, 109 (2010) 104–110.
8. Li H, Xiao HG, Yuan J, Ou J., *Compos. Part. B Eng*, 35 (2004) 185–189.
9. Son Tung Pham, *Advances in Materials Science and Engineering*, 2013, Article ID 672325, 9 pages.
10. M.J. Pellegrini-Cervantes, C.P. Barrios-Durstewitz, R.E. Nuñez-Jaquez, S.P. Arredondo-Rea, F.J. Baldenebro-Lopez, M. Rodríguez- Rodríguez, L.G. Ceballos-Mendivil, A. Castro-Beltrán, G. Fajardo-San-Miguel, F. Almeraya-Calderon, A. Martinez-Villafañe, *Int. J. Electrochem. Sci.*, 10 (2015) 332 – 346.
11. R. Puente-Ornelas, L. Chávez Guerrero, G. Fajardo-San Miguel, E. A. Rodríguez, A. Trujillo-Álvarez, H. E. Rivas-Lozano, H. M. Delgadillo-Guerra, *Int. J. Electrochem. Sci.*, 11 (2016) 277 – 290.
12. R. Siddique, Y. Aggarwal, P. Aggarwal, E.H. Kadri, R. Bennacer, *Constr. Build. Mater.*, 25 (2011) 1916–1925.
13. N.J. Saleh, R.I. Ibrahim, A.D. Salman, *Adv. Powder. Technol.*, 26 (2015) 1123–1133.
14. M. Ghrici, S. Kenai, *Cem. Concr. Comp.*, 29 (2007) 542–549.
15. F.U.A. Shaikh, S.W.M. Supit, PK. Sarker, *Mater. Des.*, 60 (2014) 433–442.
16. M. Oltulu, R. Şahin, *Mater. Sci. Eng. A.*, 528 (2011) 7012–7019.
17. M. Stefanidou, I. Papayianni, *Compos. Part B Eng.*, 43 (2012) 2706–2710.
18. F. Kontoleontos, P.E. Tsakiridis, A. Marinos, V. Kaloidas, M. Katsioti, *Constr. Build. Mater.*, 35 (2012) 347–360.
19. M. Aly, M.S.J. Hashmi, A.G. Olabi, M. Messeiry, E.F. Abadir, A.I. Hussain, *J Mater.* 33 (2012) 127-135.
20. R. Ylmén, U. Jäglid, B.M. Steenari, I. Panas, *Cem. Concr. Res.* 39 (2009) 433–439.
21. P. Hou, S. Kawashima, D. Kong, D.J. Corr, J. Qian, S.P. Shah, *Compos. Part B Eng*, 45 (2013) 440–448.
22. C. Hu, Y. Han, Y. Gao, Y. Zhang, Z. Li, *Mater. Charact.* 95 (2014) 129–139.